Available online at www.sciencedirect.com

ScienceDirect

Procedia Engineering 120 (2015) 564 – 569

Procedia Engineering

www.elsevier.com/locate/procedia

EUROSENSORS 2015

Impedance model of immune reaction leading to NETosis

Anna Schröter[a]*, Angela Rösen-Wolff[b], Gerald Gerlach[a]

[a]*Institute of Solid State Electronics, Technische Universität Dresden, 01062 Dresden, Germany*
[b]*Department of Paediatrics, University Hospital Carl Gustav Carus, Fetscherstr. 74, 01307 Dresden, Germany*

Abstract

The so-called NETs (neutrophil extracellular traps) are found in vast amounts in inflamed wounds and are therefore a good marker for wound infections. They are a product of an immune reaction. Their integrant DNA has a certain dielectric behavior due to its charge. This allows a direct electric determination without the need of a transducer. Human neutrophils were used to measure the release of NETs *in vitro*. However, the structural changes of the cells during this process have to be taken into account. In this work a model was developed which reflects these changes. This model was compared with impedance measurements. We found that changes in the medium composition strongly modify the dielectric behavior of the system. The most obvious change here is caused by the appearance of the NETs. These changes remain also stable after the cells died and did not undergo more structural changes. The measurement of NETs is a very promising approach to support the diagnosis of inflammation processes especially in wounds.

Peer-review under responsibility of the organizing committee of EUROSENSORS 2015

Keywords: wound sensor; leucocytes; dielectric cell model; impedance spectroscopy; bioimpedance

1. Introduction

Monitoring the immune status is a very important task in manifolds of clinical care situations. Human leukocytes consist of up to 50…65 % of neutrophils which play an important role for the immune defense. Neutrophils have two main immunological functions, the well-known phagocytosis and the NETosis which is a fairly newfound immune response [1]. As the name suggests it is one kind of cell death which leads to the formation of NETs. While NET aggregation is usually suppressed in the blood circulation by nucleases [2], they especially accumulate in

* Corresponding author. Tel.: +0-049-351-463-34171; fax: +0-049-351-463-32320.
E-mail address: anna.schroeter@tu-dresden.de

Peer-review under responsibility of the organizing committee of EUROSENSORS 2015
doi:10.1016/j.proeng.2015.08.724

inflamed wounds. These aggregates are visible as pus in the wound [3]. Furthermore, NETs play an important role in many inflammatory and autoimmune disorders [4]. They consist mainly of DNA from the sacrificed neutrophils which elongate and form a trap to catch pathogens and avoid their immigration to the host. The massive appearance and the unspecific and fast activation make NETs an excellent inflammation marker during wound healing. Due to its molecular structure DNA is negatively charged. These large, charged molecules can be electrically detected without the need of a transducer. In previous works we have shown the possibility to monitor the NET formation of human neutrophils with impedimetric sensors [5, 6]. However, we faced the problem that we had not been able to separate the signal caused by the enrichment of NETs and by structural changes of the cells. To overcome this difficulty, we present here a physical model reflecting the dielectric properties of neutrophils during the diverse steps of NET formation. Afterwards, the model is compared with real measurements on cells.

Nomenclature

symbols			***subscripts***
A	depolarisation factor	c	cell
a, b, c	half axis of ellipsoid in x, y, z direction	cp	cytoplasm
d	thickness of membrane	i	interior of particle
f	frequency	k	room direction (x,y,z)
P	volume fraction of cells or particles in medium	M	medium
R	radius	m	cell membrane
t	half axis	n	nuclear
$\underline{\varepsilon}$	complex relative permittivity, $\underline{\varepsilon} = \varepsilon + \mathrm{j}\,\kappa$	nm	nuclear membrane
ν	geometrical parameter	np	nucleoplasm
ξ	ellipsoidal coordinate	p	boundary layer
constants		s	shell
j	imaginary unit ($j^2 = -1$)		
ε_0	vacuum permittivity ($8.85 \cdot 10^{-12}$ F/m)		

2. Theory

2.1. Steps of NETosis

The appearance of neutrophils is schematically drawn in Figure 1a. A typical property is the segmented cell core consisting of 2…5 lobes. The values of the showed properties are summarized in Table 1. Upon activation with bacteria or a chemical stimulant, e.g. phorbol 12-myristate 13-acetate (PMA), neutrophils undergo certain morphological changes. These changes, which influence the dielectric properties of the neutrophil suspension, are shown in Figure 1b. After a short ruffling of the surface the cell gets round again. In a natural environment the neutrophil granulocyte attaches to the blood vessel wall and starts migrating to the infection site. The attachment, attended by a volume increase and flattening of the whole cell, can also be seen with PMA stimulation. Simultaneously, the nucleus grows and loses his lobes. After the nucleus fills nearly the entire cell interior the nuclear membrane starts disintegrating. Nuclear and cytoplasmic material mixes and is released after the cell membrane dissolved. The nuclear-cytoplasmic mixture spreads as web-like structures: the NETs.

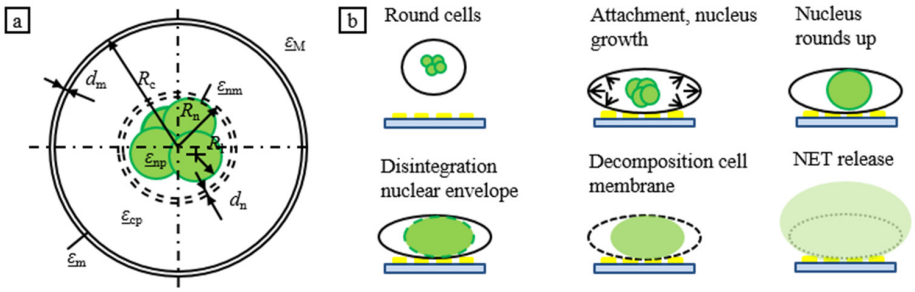

Fig. 1. (a) geometrical assembly of neutrophil parts with their radii, thicknesses and corresponding permittivity; (b) schematic steps of NETosis after PMA stimulation [7, 8].

Table 1. Values for unactivated neutrophils. * are own measurements.

Parameter	ε_M	κ_M (S/m)	ε_m	κ_m (S/m)	ε_{cp}	κ_{cp} (S/m)	ε_{nm}	κ_{nm} (S/m)	ε_{np}	κ_{np} (S/m)	d_m (nm)	d_n (nm)	R_c (µm)	R_n (µm)	R_l (µm)
Value	78.2	1.3	6.2	$1 \cdot 10^{-12}$	60	0.3	28	$6 \cdot 10^{-3}$	52	0.135	8	9	4.5	3.5	1.5
Source	*	*	[9]	[9]	[9]	[9]	[10]	[10]	[10]	[10]	[10]	[10]	[11]	[12]	*

2.2. Dielectric properties of cells

To model the steps of NET formation from Figure 1a, a physical description is helpful. Asami *et al.* proposed dielectric models for biological cells [10, 13] which were also used by Griffith *et al.* to model neutrophils for electrorotation experiments after PMA stimulation [14]. The latter group reported slight disagreements between model and measurements. One reason could be that they did not consider the changes of the nucleus and flattening of the cell. The flattening of the cell can be modeled by using the equation for the resulting permittivity of a suspension $\underline{\varepsilon}$ of shelled oblate particles with the half axes $a \neq b = c$ and the volume fraction P in medium with the permittivity $\underline{\varepsilon}_M$ derived by Asami *et al.* [10]:

$$\frac{\underline{\varepsilon} - \underline{\varepsilon}_M}{\underline{\varepsilon} + 2\underline{\varepsilon}_M} = \frac{1}{9} P \sum_{k=x,y,z} \frac{\underline{\varepsilon}_k - \underline{\varepsilon}_M}{\underline{\varepsilon}_M + (\underline{\varepsilon}_k - \underline{\varepsilon}_M) A_{0k}} \tag{1}$$

where $\underline{\varepsilon}_k$ is the equivalent permittivity of particle with a thin shell and its interior in each direction of space:

$$\underline{\varepsilon}_k = \underline{\varepsilon}_s \frac{\underline{\varepsilon}_s + (\underline{\varepsilon}_i - \underline{\varepsilon}_s) A_{1k} + \nu (\underline{\varepsilon}_i - \underline{\varepsilon}_s)(1 - A_{0k})}{\underline{\varepsilon}_s + (\underline{\varepsilon}_i - \underline{\varepsilon}_s) A_{1k} - \nu (\underline{\varepsilon}_i - \underline{\varepsilon}_s) A_{0k}} \tag{2}$$

with the permittivity of the shell $\underline{\varepsilon}_s$ and the interior $\underline{\varepsilon}_i$. The geometrical parameters are defined as

$$\nu = \frac{(a-d)(b-d)^2}{ab^2} \tag{3}$$

$$A_{pk} = ab^2 \int_0^\infty \frac{\mathrm{d}\xi}{\left(t_p{}^2 + \xi\right)\sqrt{\left(\xi + a^2\right)\left(\xi + b^2\right)^2}} \tag{4}$$

where $t_p = a, b, c$ is the half axis in the x, y, z direction accordingly. The subscript p marks the outer (0) or inner (1) boundary layer. For the half axes of round particles holds $a = b$. Insertion of this condition in equation (1) and (2) leads to Hanai's mixture equation [15] and one equation for spherical shelled particles derived by Hanai *et al.* before [16].

3. Methods

3.1. Modeling

The modeling is done with Matlab Version R2014b. With equation (1-4) many parameter changes during NETosis can be simulated by adjusting the geometrical parameters. However, due to the cubic root of complex numbers, it is difficult to obtain pure analytical results, especially for Equation (1) and Hanai's mixture equation derived from it. This was solved by using the iterative Müller's method. All the other equations were solved by inbuilt Matlab standard functions. Table 2 shows the adjustments which were used to model NET formation. Step 1

marks the starting point with round cells and a lobed cell core. Step 2 connects several sub steps like the flattening of the cells and nucleus, the loss of lobes leading to an oblate cell core, the volume increase of both cells and cell cores and the adherence leading to a higher volume fraction in proximity of the planar electrodes. In the last steps, the dissolving of nuclear and cellular membrane leads to the disappearance of the dielectric phenomena caused by them. Consequently, they were erased. The parameter changes are estimated freely and partly from microscopic observations.

Table 2. Temporary course of NETosis after PMA stimulation.

Event	Stimulation time in h:min	Model adjustment	Numeration
Round cells	0:05	Cells: shelled spherical particle, nuclei: 4 shelled particles in nuclear area, starting values (Table 1), $P = 0.31$	1
Flattening, cells extend out, nucleus spread out, attachment [7]	0:30	Cells: oblate ellipsoids, $a_c = 2.6$ µm, $b_c = R_c = 8$ µm half axis increases, nuclear radius increase, increase of cell volume fraction, $P = 0.74$	2
Nuclei start losing lobules, expend, fill almost cell interior [8] some nucleus round [7]	1:00 1:20 2:00	Nuclei: oblate, $a_n = 2.4$ µm, $b_n = R_n = 7$ µm	2
Nuclear envelop starts disintegrating, mixing of nucleoplasm and cytoplasm [7, 8]	3:00	Erase of nuclei	3
Rupture of plasma membrane [8], All nucleus spherical [7], Nearly all cells dead [7]	3:40 4:00 6:00	Erase of cells	4

3.2. Cell preparation and impedance measurements

The neutrophils were prepared as described in [5] but with some modifications. We used PolymorphPrep (Axis-Shield) for density gradient centrifugation for higher yield and better cell protection. The RPMI medium contained HEPES buffer (100 mM), Penicillin/Streptomycin (1 %) and this time 10 % heat-inactivated (70°C) fetal calf serum to avoid NET decomposition by nucleases. Some $2 \cdot 10^6$ cells were seeded on the interdigitated electrodes of the E-Plate 16 (Applied Biosciences) coated with poly-L-lysine. Stimulation with PMA was done in an analogous manner.

Impedance measurements were also performed as before [5] with a self-made adapter connected to the impedance analyzer ISX-3 (Sciospec). A calibration procedure was introduced to filter out parasitic circuit elements like cable inductance, resistance and capacitance for every well and to find the geometric constant of electrode arrangement (12.56). The equivalent circuit corresponds to that one in [17]. Also the permittivity was calculated as in [17]. The measurement range was expanded to 10 MHz starting from 100 Hz in 30 steps to reveal changes in the higher frequency range. The voltage amplitude was kept at 12 mV. The measurement included one reference spectrum before stimulation and the continuous recording after stimulation for 8 hours.

4. Results

The results of the simulation of NETosis are shown in Figure 2a. On purpose we just modeled the cell structural behavior itself. The steps correspond to the numeration in Table 2. Step 1 starts with round cells with a lobed cell core. One dispersion is clearly visible at a cut-off frequency of 2 MHz and characterizes the interfacial polarization of the cell membrane. The other dispersion caused by the nuclear lobes is at about 100 MHz and is slightly visible in the conductivity spectrum. Step 2 includes a volume increase which would lead to a decrease of the cut-off frequency. The simultaneous flatting which was simulated by an oblate ellipsoid and leads to a broader dispersion due to two relaxations along the two different half axes. The cut-off frequencies amount to 1 MHz and 90 MHz, respectively. The dissolving of the cell core in step 3 is hardly distinguishable because its dimensions are in the

range of the cell itself. Dissolving of the cell membrane, modeled simply by erasing the cell structure, leads to the spectrum of the medium.

The measurement revealed different pictures (Figure 2b). The medium shows a high permittivity of ca. 100,000 and a dispersion starting at 100 kHz. At 500 kHz the spectra show discontinuities which cannot arise from real physical phenomena but seem to be a measurement artefact. The measurement values strengthen this argumentation with negative real parts of the impedance. This is also the reason why we were not able to measure values 1 MHz. The manufacturer confirmed a problem with the calibration procedure of the device which we could not resolve up to now. A drop in the permittivity in the high frequency range occurs for cells after 5 minutes of stimulation. During further progress of the stimulation it decreases mostly at ca. 20 kHz. Interestingly, a short phase of increase of the permittivity occurs after 2 h until it falls back to the initial value after 3 hours. After 6 h the value remains constant.

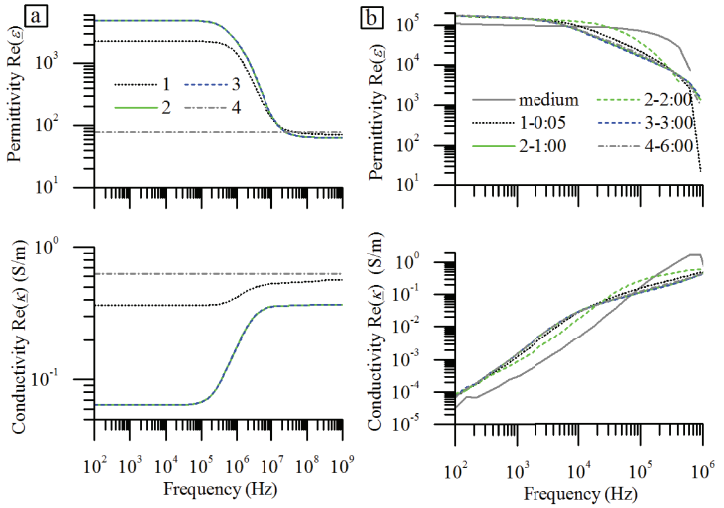

Fig. 2. (a) permittivity and conductivity spectra of the NETosis model comprising steps 1, 2, 3 and 4 corresponding to Table 2; (b) representative measured spectra of cells with certain time points related to the steps of NETosis (in the legend: step - stimulation time).

5. Discussion

The model shows a general increase of the permittivity caused by the volume increase of the cells in the lower and medium frequency range. This was not confirmed by the measurement results where, contrarily, the permittivity droped. Furthermore it is obvious that the starting permittivity values with cells is much higher than that one in the simulation. First, we did not consider proteins in the basic medium, which can slightly increase the permittivity. We assume that this difference between the simulated and measured values might arise from the electrode polarization. This assumption is supported by the fact that the pure medium measurement shows already the lower tail of a dispersion probably caused by electrode polarization. Electrode polarization can have a masking effect on cell measurements which makes it difficult to reveal structural changes of the cell [17]. Nevertheless, it depends strongly on the properties of the medium which explains why there are still changes visible during NET formation around 20 kHz.

A lower conductivity leads to a decrease of the cut-off frequency. As it can be seen in the spectra of the Figure 2b the conductivity slightly decreases in this range with cell activation. This decrease can be caused by the fast attachment of the neutrophils in proximity of the electrodes. The volume increase is a slower process continuing after attachment [3] which could explain the intermediate increase after 2 hours as supported also by the model. The model did not include the changes of the medium composition, especially of the mixing of the nuclear material with the cell interior and also the mixing of cell medium with the cytoplasmic-nuclear constituent and namely of the NETs. The fact that the permittivity remains constant after cell death (6 h) means that the medium changed its

properties clearly. This is also visible in the impedance spectra (not shown) and stands in contrast to our earlier measurements [5], where we used autologous serum which contains nucleases that cleave the DNA of NETs. In this experiments the signal remained stable until 8 hours – a very long time after cell death.

6. Conclusions

A model is presented that reflects the structural properties of neutrophils. With this model it was possible to simulate several morphological changes during NETosis which also lead to the modification of the equivalent dielectric properties of the cell suspension. The volume increase and flattening of the cells leads to a permittivity increase which was also visible in the measurements. Modifications of the medium composition were not simulated due to the lack of corresponding data. This will be done in the next steps. Not all effects of the simulated permittivity changes were visible in the measured spectra. The main reason for that was the masking effect of the electrode polarization. Because the electrode polarization is dependent on medium composition, effects of changes of the medium can be seen. As it is expected, the NETs can influence the medium properties decisively. This assumption is also supported by the fact that the permittivity decrease around 20 kHz remain stable after cell death.

Acknowledgements

This work was done in the frame of the project “Textiles Wundmonitoring” (IGF project 17826 BR of the research alliance Forschungskuratorium Textil e.V.) and was funded by AiF in the frame of the Program for Facilitation of Industrial Corporative Research (IGF) of the Bundesministerium für Wirtschaft und Technologie based on a resolution of the Deutscher Bundestag. The authors would like to thank for the financial support.

References

[1] V. Brinkmann, U. Reichard, C. Goosmann *et al.*, Neutrophil Extracellular Traps Kill Bacteria, Science. 303 (5663:2004), 1532–1535.
[2] M. von Köckritz-Blickwede, O. A. Chow, V. Nizet, Fetal calf serum contains heat-stable nucleases that degrade neutrophil extracellular traps, Blood. 114 (25:2009), 5245–5246.
[3] V. Brinkmann, A. Zychlinsky, Beneficial suicide: why neutrophils die to make NETs, Nat. Rev. Micro. 5 (8:2007), 577–582.
[4] M. J. Kaplan, M. Radic, Neutrophil Extracellular Traps: Double-Edged Swords of Innate Immunity, J. Immunol. 189 (6:2012), 2689–2695.
[5] A. Schröter, G. Gerlach, A. Rösen-Wolff, Impedance Measurement of Wound Infection Status, in: AMA Service GmbH (Ed.), Proceedings SENSOR 2013, 2013, 628–632.
[6] A. Schröter, A. Rösen-Wolff, G. Gerlach, Impedance-based detection of extracellular DNA in wounds, JPCS, 434 (1:2013), 12057.
[7] H. Takei, A. Araki, H. Watanabe *et al.*, Rapid killing of human neutrophils by the potent activator phorbol 12-myristate 13-acetate (PMA) accompanied by changes different from typical apoptosis or necrosis, J. Leukoc. Biol. 59 (2:1996), 229–240.
[8] T. A. Fuchs, U. Abed, C. Goosmann *et al.*, Novel cell death program leads to neutrophil extracellular traps, J. Cell Biol. 176 (2:2007), 231–241.
[9] H. Ziervogel, R. Glaser, D. Schadow *et al.*, Electrorotation of lymphocytes-the influence of membrane events and nucleus, Bioscience Rep. 6 (1986), 973–982.
[10] K. Asami, Y. Takahashi, S. Takashima, Dielectric properties of mouse lymphocytes and erythrocytes, BBA-Mol. Cell Res. 1010 (1:1989), 49–55.
[11] D. Zucker-Franklin, M. F. Greaves, C. E. Grossi *et al.*, Neutrophils, in: Zucker-Franklin, D. (Eds.), Atlas of Blood Cells: Function and Pathology, Lea & Febiger, Philadelphia, 1988.
[12] B. H. Davis, R. J. Walter, C. B. Pearson *et al.*Membrane activity and topography of F-Met-Leu-Phe-Treated polymorphonuclear leukocytes. Acute and sustained responses to chemotactic peptide, Am. J. Pathol. 108 (2:1982), 206.
[13] K. Asami, T. Hanai, N. Koizumi, Dielectric Approach to Suspensions of Ellipsoidal Particles Covered with a Shell in Particular Reference to Biological Cells, Jpn. J. Appl. Phys. 19 (2:1980), 359.
[14] A. W. Griffith, J. M. Cooper, Single-Cell Measurements of Human Neutrophil Activation Using Electrorotation, Anal. Chem. 70 (13:1998), 2607–2612.
[15] T. Hanai, Theory of the dielectric dispersion due to the interfacial polarization and its application to emulsions, Kolloid Z. 171 (1:1960), 23-31.
[16] T. Hanai, K. Asami, N. Koizumi, Dielectric theory of concentrated suspensions of shell-spheres in particular reference to the analysis of biological cell suspensions, Bull. Inst. Chem. Res. Kyoto Univ. 57 (1979), 297–305.
[17] F. Bordi, C. Cametti, T. Gili, Reduction of the contribution of electrode polarization effects in the radiowave dielectric measurements of highly conductive biological cell suspensions, Bioelectrochemistry. 54 (1:2001), 53–61.